strictly above 1.4×10^4 $M_\odot$ AU^{-3}. The dynamical lifetime of a cluster of objects with that density would be less than 1000 years, making Sgr A* the most convincing existing case for a massive black hole (*39*).

References and Notes

1. F. Melia, H. Falcke, *Annu. Rev. Astron. Astrophys.* **39**, 309 (2001).
2. A. M. Ghez *et al.*, *Astrophys. J.* **586**, 127L (2003).
3. R. Schödel *et al.*, *Astrophys. J.* **596**, 1015 (2003).
4. H. Falcke *et al.*, *Astrophys. J.* **499**, 731 (1998).
5. R. Genzel *et al.*, *Nature* **425**, 934 (2003).
6. A. M. Ghez *et al.*, *Astrophys. J.* **601**, 159L (2004).
7. F. K. Baganoff *et al.*, *Nature* **413**, 45 (2001).
8. G. C. Bower, H. Falcke, R. J. Sault, D. C. Backer, *Astrophys. J.* **571**, 843 (2002).
9. G. C. Bower, M. C. H. Wright, H. Falcke, D. C. Backer, *Astrophys. J.* **588**, 331 (2003).
10. H. Falcke, F. Melia, E. Agol, *Astrophys. J.* **528**, 13L (2000).
11. W. Goss, R. Brown, K. Lo, *Astron. Nachr.* **324** (suppl.), 497 (2003).
12. T. J. W. Lazio, J. M. Cordes, *Astrophys. J.* **505**, 715 (1998).
13. R. Narayan, J. Goodman, *Mon. Not. R. Astron. Soc.* **238**, 963 (1989).
14. P. N. Wilkinson, R. Narayan, R. E. Spencer, *Mon. Not. R. Astron. Soc.* **269**, 67 (1994).
15. K. M. Desai, A. L. Fey, *Astrophys. J. Supp. Ser.* **133**, 395 (2001).
16. A. S. Trotter, J. M. Moran, L. F. Rodriguez, *Astrophys. J.* **493**, 666 (1998).
17. K. Y. Lo, Z. Q. Shen, J. H. Zhao, P. T. P. Ho, *Astrophys. J.* **508**, 61L (1998).
18. We assume for Sgr A* a black hole mass of 4×10^6 $M_\odot$ and a distance of 8.0 kpc (*2*). The latter implies that 0.1 milli–arc sec = 0.8 AU = 1.1×10^{13} cm. Together, these quantities imply a Schwarzschild radius $R_s = 2GM/c^2 = 1.2 \times 10^{12}$ cm = 0.08 AU = 0.01 milli–arc sec, where G is Newton's gravitational constant.
19. S. S. Doeleman *et al.*, *Astron. J.* **121**, 2610 (2001).
20. R. Herrnstein, J.-H. Zhao, G. C. Bower, W. M. Goss, *Astron. J.*, in press.
21. G. C. Bower, D. C. Backer, R. A. Sramek, *Astrophys. J.* **558**, 127 (2001).
22. E. W. Greisen, *Information Handling in Astronomy: Historical Vistas* (Kluwer Academic Publishers, Dordrecht, Netherlands, 2003), pp. 109–126.
23. A. E. E. Rogers, S. S. Doeleman, J. M. Moran, *Astron. J.* **109**, 1391 (1995).
24. A. R. Thompson, J. M. Moran, G. W. Swenson, *Interferometry and Synthesis in Radio Astronomy* (Wiley, New York, 2001).
25. L98 determined a scattering law $\sigma_{axis} = \sigma^{1cm}_{axis} \lambda^{\alpha}_{axis}$, where axis is either major or minor, λ is given in cm, $\sigma^{1cm}_{major} = 1.43 \pm 0.02$ milli–arc sec, and $\sigma^{1cm}_{minor} = 0.76 \pm 0.05$ milli–arc sec. α is the index of the scattering law and it is assumed to be 2 for the strong scattering case. L98 found $\alpha_{major} = 1.99 \pm 0.03$. The major axis is oriented almost purely east-west at a position angle of 80° east of north.
26. F. Yusef-Zadeh, W. Cotton, M. Wardle, F. Melia, D. A. Roberts, *Astrophys. J.* **434**, 63L (1994).
27. T. Beckert, W. J. Duschl, *Astron. Astrophys.* **328**, 95 (1997).
28. R. D. Blandford, A. Konigl, *Astrophys. J.* **232**, 34 (1979).
29. H. Falcke, S. Markoff, *Astron. Astrophys.* **362**, 113 (2000).
30. F. Melia, *Astrophys. J.* **426**, 577 (1994).
31. R. Narayan, R. Mahadevan, J. E. Grindlay, R. G. Popham, C. Gammie, *Astrophys. J.* **492**, 554 (1998).
32. F. Yuan, E. Quataert, R. Narayan, *Astrophys. J.* **598**, 301 (2003).
33. M. E. Nord, T. J. W. Lazio, N. E. Kassim, W. M. Goss, N. Duric, *Astrophys. J.* **601**, 51L (2004).
34. J. Zhao *et al.*, *Astrophys. J.* **586**, L29 (2003).
35. A. Broderick, R. Blandford, *Mon. Not. R. Astron. Soc.* **342**, 1280 (2003).
36. D. C. Backer, R. A. Sramek, *Astrophys. J.* **524**, 805 (1999).
37. M. J. Reid, A. C. S. Readhead, R. C. Vermeulen, R. N. Treuhaft, *Astrophys. J.* **524**, 816 (1999).
38. M. Reid *et al.*, *Astron. Nachr.* **324**, S1 (2003).
39. E. Maoz, *Astrophys. J.* **494**, 181L (1998).

40. The National Radio Astronomy Observatory is a facility of NSF, operated under cooperative agreement by Associated Universities, Incorporated.

Supporting Online Material
www.sciencemag.org/cgi/content/full/1094023/DC1
SOM Text
Figs. S1 to S4
Tables S1 to S3
References

25 November 2003; accepted 22 March 2004
Published online 1 April 2004;
10.1126/science.1094023
Include this information when citing this paper.

REPORTS

In-Plane Spectral Weight Shift of Charge Carriers in $YBa_2Cu_3O_{6.9}$

A. V. Boris,* N. N. Kovaleva,† O. V. Dolgov, T. Holden,‡ C. T. Lin, B. Keimer, C. Bernhard

The temperature-dependent redistribution of the spectral weight of the CuO_2 plane–derived conduction band of the $YBa_2Cu_3O_{6.9}$ high-temperature superconductor (superconducting transition temperature = 92.7 kelvin) was studied with wide-band (0.01– to 5.6–electron volt) spectroscopic ellipsometry. A superconductivity-induced transfer of the spectral weight involving a high-energy scale in excess of 1 electron volt was observed. Correspondingly, the charge carrier spectral weight was shown to decrease in the superconducting state. The ellipsometric data also provide detailed information about the evolution of the optical self-energy in the normal and superconducting states.

The mechanism of high-temperature superconductivity (HTSC) is one of the main unsolved problems in condensed-matter physics. An influential class of theories predicts that HTSC arises from an unconventional pairing mechanism driven by a reduction of the kinetic energy of the charge carriers in the superconducting (SC) state (*1*–*3*). This contrasts with the conventional Bardeen-Cooper-Schrieffer (BCS) model, where correlations of the charge carriers below the SC transition temperature, T_c, bring about an increase in their kinetic energy (*4*, *5*), which is overcompensated for by a reduction of the potential energy due to the phonon-mediated attraction. Within a nearest-neighbor tight-binding model, measurements of the optical conductivity $\sigma_1(\omega) = Re[\sigma(\omega)]$ can provide experimental access to the kinetic energy $\langle K \rangle$ via the sum rule for the spectral weight $SW(\tilde{\Omega}) = \int_0^{\tilde{\Omega}} \sigma_1(\omega) d\omega = \frac{\pi e^2 a^2}{2\hbar^2 V_u} \langle -K \rangle$, where a is the in-plane lattice constant and V_u is the unit cell volume (*3*, *6*–*8*). The upper integration limit, $\tilde{\Omega}$, needs to be high enough to include all transitions within the conduction band but sufficiently low to exclude the interband transitions.

Precise optical data may thus enable one to address the issue of a kinetic energy–driven HTSC pairing mechanism. In fact, optical measurements have ruled out a lowering of the kinetic energy along the c axis (perpendicular to the highly conducting CuO_2 planes) as the sole mechanism of HTSC (*9*), but have also shown that it can contribute significantly to the superconducting condensation energy of multilayer copper oxides (*10*, *11*). Recently, experimental evidence for an alternative mechanism driven by a reduction of the in-plane kinetic energy (*3*) has been reported (*12*, *13*). The comprehensive data set presented here, however, demonstrates that this scenario is not viable.

We performed direct ellipsometric measurements of the complex dielectric function $\varepsilon(\omega) = \varepsilon_1(\omega) + i\varepsilon_2(\omega) = 1+$

Max-Planck-Institut für Festkörperforschung, Heisenbergstrasse 1, D-70569 Stuttgart, Germany.

*To whom correspondence should be addressed. E-mail: A.Boris@fkf.mpg.de
†Also at the Institute of Solid State Physics, Russian Academy of Sciences, Chernogolovka, Moscow district, 142432 Russia.
‡Present address: Department of Physics, Brooklyn College of the City University of New York, Brooklyn, NY 11210, USA.

$4\pi i\sigma(\omega)/\omega$ over a range of photon energies extending from the far infrared ($\hbar\omega = 0.01$ eV) into the ultraviolet ($\hbar\omega = 5.6$ eV) (*8*). We focus here on the *a*-axis component of $\varepsilon(\omega)$ of a detwinned $YBa_2Cu_3O_{6.9}$ crystal at optimum doping ($T_c = 92.7 \pm 0.4$ K) (*8*). In agreement with previous reports (*12*–*15*), we observed a SC-induced transfer of SW involving an unusually high energy scale in excess of 1 eV. However, our data provide evidence for a SC-induced decrease of the intraband SW and are thus at variance with models of in-plane kinetic energy–driven pairing. Additional data along the *b* axis of the same crystal and for slightly underdoped $Bi_2Sr_2CaCu_2O_8$ ($T_c = 86 \pm 0.5$ K) supporting these conclusions are presented in the supporting online text and figures.

Figure 1, A and B, shows the difference spectra $\Delta\sigma_{1a}(\omega)$ and $\Delta\varepsilon_{1a}(\omega)$ for the normal and SC states (the measured spectra are displayed in fig. S1). Figure 1, C to F, details the temperature dependence of σ_{1a} and ε_{1a}, averaged over different representative photon energy ranges.

First we discuss the *T*-dependent changes in the normal state. The most important observation is the smooth evolution of $\Delta\sigma_{1a}(\omega)$ and $\Delta\varepsilon_{1a}(\omega)$ over an energy range of at least 0.1 to 1.5 eV. The additional features in $\Delta\sigma_{1a}(\omega)$ and $\Delta\varepsilon_{1a}(\omega)$ above 1.5 eV arise from the *T*-dependent evolution of the interband transitions (*16*, *17*). Apparently, the response below 1.5 eV is featureless and centered at very low frequency below 50 meV. It can hence be ascribed to a Drude peak [due to transitions within the conduction band or a narrowly spaced set of conduction bands (*18*)] whose tail at high energy is significantly enhanced by inelastic interaction of the charge carriers. A narrowing of the broad Drude peak at low *T* accounts for the characteristic *T*-dependent SW shift from high to low energies, while it leaves the intraband SW unaffected (*19*). SW is removed from the high-energy tail, which involves a surprisingly large energy scale of more than 1.5 eV, and transferred to the "head" near the origin. As a consequence, $\sigma_{1a}(\omega)$ curves at different temperatures intersect; for instance, around $\omega \sim 20$ meV for $\sigma_{1a}(\omega)$ curves at 200 and 100 K [inset of fig. S1A]. Furthermore, as detailed in the online material, the integration of $\Delta\sigma_{1a}(\omega)$ above the intersection point yields a SW loss that is well balanced by the estimated SW gain below the intersection point, so that the total SW is conserved within the experimental error.

The *T* dependence of ε_{1a} affords an independent and complementary way to analyze the SW shift from high to low energies. Figure 1 shows that σ_{1a} and ε_{1a} follow the same *T* dependence in the normal state; that is, a concomitant decrease of both quantities with decreasing *T* is observed at every energy over a wide range from 0.05 to 1.5 eV. A simple analysis of these data based on the Kramers-Kronig (KK) relation (*20*) confirms that the SW lost at high energies is transferred to energies below 0.1 eV. We note that the blue shift of the zero-crossing of ε_{1a}, $\omega|_{\varepsilon_1=0}$ (inset of fig. S1B), can be explained by the narrowing of the broad Drude peak alone, without invoking a change of the total intraband SW.

We now turn to the central issue, the evolution of the SW in the SC state. It can be seen in Fig. 1 that the *T*-dependent decrease of σ_{1a} in the high-energy range becomes even more pronounced in the SC state. The data of Fig. 1, E and F, thus confirm previous reports of an anomalous SC-induced SW decrease at high energies (*12*, *13*). Figure 1, C and D, however, show that this trend continues down to at least 0.15 eV, and Fig. 1A reveals that the difference spectra $\Delta\sigma_{1a}$ do not differ substantially between normal and SC states in the energy range between 0.15 and 1.5 eV. In both cases, $\Delta\sigma_{1a}$ exhibits a continuous decrease toward high energy, which levels off near 1.5 eV. As discussed above, this behavior is characteristic of the narrowing of a broad intraband response. Significant differences between the responses in the normal and SC states are observed only below ~0.15 eV, where the SC-induced changes are dominated by formation of the SC condensate. The latter effect has been extensively discussed in the literature (*8*, *21*).

Next we discuss the evolution of the real part of the dielectric function, ε_{1a}, in the SC state, which again provides complementary information about the SW redistribution. For the normal state, we have shown that the transfer of SW from high to low energies gives rise to a decrease of $\varepsilon_{1a}(\omega)$, as dictated by the KK relation between $\varepsilon_{1a}(\omega)$ and $\sigma_{1a}(\omega)$. Figure 1 shows that this trend suddenly ceases in the SC state, where ε_{1a} does not exhibit a SC-induced anomaly mirroring the one of σ_{1a}. Whereas σ_{1a} decreases precipitously below T_c, ε_{1a} remains virtually *T*-independent. This trend holds not only near $\omega|_{\varepsilon_1=0} \sim 0.9$ eV but persists over a wide energy range from 1.5 eV down to at least 0.15 eV. The KK relation necessarily implies that the SW loss between 0.15 and 1.5 eV needs to be balanced by a corresponding SW gain below 0.15 eV and above 1.5 eV (*8*, *20*). In addition to the SW transfer to low energies due to the narrowing of the charge carrier response, as discussed above, the SC-induced SW change must therefore involve the shift of a significant amount of SW from low energy ($\omega < \omega|_{\varepsilon_1=0}$) to energies well in excess of $\omega|_{\varepsilon_1=0}$. In contrast to the situation in the normal state, where the total charge carrier SW is conserved within the experimental uncertainty, this additional SC-induced shift of SW to high energies gives rise to a decrease of the total charge carrier SW. We emphasize that this is a model-independent conclusion based solely on the KK relation (*8*, *20*) between $\varepsilon_{1a}(\omega)$ and $\sigma_{1a}(\omega)$, both of which are directly measured by ellipsometry.

The related SW changes can be quantified using the extended Drude formalism, where the

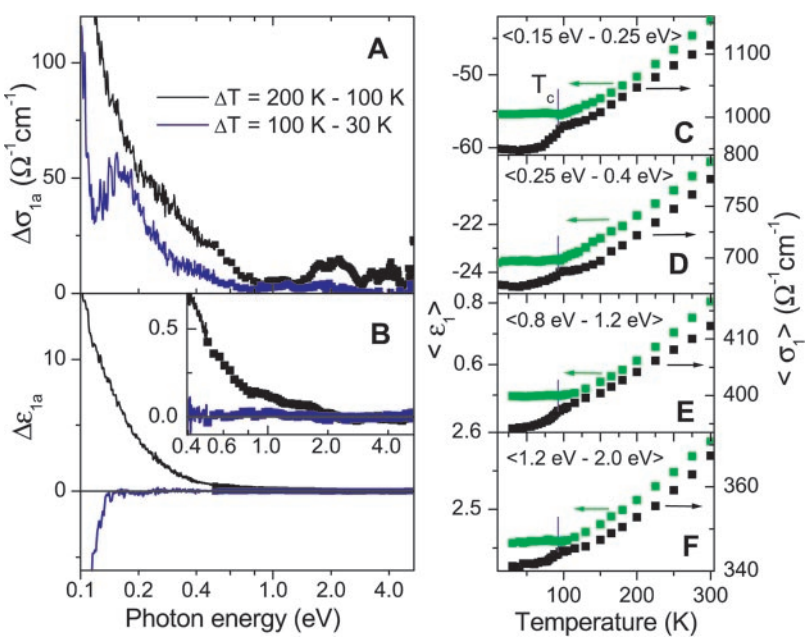

Fig. 1. Difference spectra (**A**) $\Delta\sigma_{1a}(\omega) = \sigma_{1a}(T_2,\omega) - \sigma_{1a}(T_1,\omega)$ and (**B**) $\Delta\varepsilon_{1a}(\omega) = \varepsilon_{1a}(T_2,\omega) - \varepsilon_{1a}(T_1,\omega)$ in the normal state at $T_1 = 100$ K and $T_2 = 200$ K and below the SC transition between $T_1 = 30$ K ($<T_c$) and $T_2 = 100$ K ($\gtrsim T_c$). The inset in (B) provides an enlarged view of $\Delta\varepsilon_{1a}(\omega)$ over the photon energy range from 0.4 to 4 eV. (**C** to **F**) Temperature dependence of $\sigma_{1a}(\omega)$ (black squares) and $\varepsilon_{1a}(\omega)$ (green squares) averaged over different energy ranges.

real and imaginary parts of the optical self-energy, $\Sigma(\omega)$, are represented by a frequency-dependent mass-renormalization factor, $m^*(\omega)/m_b$, and scattering rate, $\gamma(\omega)$, respectively (*8*). The renormalized plasma frequency

$$\omega^*_{pl}(\omega) = \omega_{pl}\sqrt{\frac{m_b}{m^*(\omega)}} = \omega\sqrt{\frac{\varepsilon_2^2(\omega) + (\varepsilon_\infty - \varepsilon_1(\omega))^2}{\varepsilon_\infty - \varepsilon_1(\omega)}} \quad (1)$$

and the scattering rate

$$\gamma(\omega) = \frac{\omega_{pl}^2}{\omega}\frac{\varepsilon_2(\omega)}{\varepsilon_2^2(\omega) + (\varepsilon_\infty - \varepsilon_1(\omega))^2} = \omega_{pl}^2 \times f[\varepsilon_1(\omega), \varepsilon_2(\omega)] \quad (2)$$

can be derived from the ellipsometric data. The value of $\varepsilon_\infty = 5 \pm 1$ is extracted from the high-energy part of the spectra (*22*). The normalized difference between normal and SC states, $\Delta\omega^*_{pl}(\omega)/\omega^*_{pl}(\omega)$, is displayed in Fig. 2A (*23*). Most notably, $\Delta\omega^*_{pl}(\omega)/\omega^*_{pl}(\omega)$ saturates above 0.3 eV at a finite value of ~0.5% (thin red line). This finite asymptotic value of $\Delta\omega^*_{pl}(\omega)/\omega^*_{pl}(\omega) \equiv \Delta\omega_{pl}/\omega_{pl} - 1/2 \times \Delta(m^*(\omega)/m_b)/(m^*(\omega)/m_b)$ above 0.3 eV cannot be ascribed to an anomaly of the mass-renormalization factor $\Delta(m^*(\omega)/m_b)$, which should decrease to zero as a function of increasing energy. Instead, the asymptotic value of $\Delta\omega^*_{pl}/\omega^*_{pl}$ ($\omega > 0.3$) is indicative of a SC-induced change in the bare plasma frequency, ω_{pl}. With $\omega_{pl} = 2.04 \pm 0.04$ eV, as derived from $\omega^*_{pl}(\omega)$ (inset of Fig. 2A) around 0.45 eV, and $SW(\tilde{\Omega}) = \omega^2_{pl}/8$ we thus obtain a SC-induced loss of the intraband SW of $\Delta SW = 5.2 \pm 0.7 \times 10^{-3}$ eV^2.

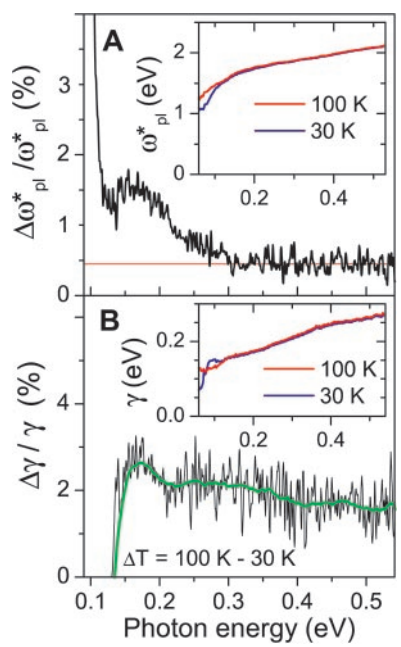

Fig. 2. Normalized difference of (**A**) $\Delta\omega^*_{pl}(\omega)/\omega^*_{pl}(\omega)$ and (**B**) $\Delta\gamma(\omega)/\gamma(\omega)$, defined in the text, upon heating from 30 to 100 K. The green curve results from smoothing of the experimental data (light black line). The insets show (A) $\omega^*_{pl}(\omega)$ and (B) $\gamma(\omega)$ at 30 K ($<T_c$) and 100 K ($\gtrsim T_c$).

Figure 2B shows the normalized difference $\Delta\gamma(\omega)/\gamma(\omega) \equiv 2 \times \Delta\omega_{pl}/\omega_{pl} + \Delta f(\omega)/f(\omega)$, with $\Delta\omega_{pl}/\omega_{pl} = 0.5\%$ and $\Delta f(\omega)/f(\omega)$ derived directly from the data (*23*). The anomaly of the scattering rate evidently extends to very high energy, exhibiting a slow but steady decrease with increasing energy. In contrast, the SC-induced anomaly in the mass-renormalization factor decreases rapidly and essentially vanishes above 0.3 eV. This decrease of $Re[\Sigma(\omega)]$ with an energy scale of ~0.3 eV provides an upper limit for the spectrum of excitations strongly coupled to the charge carriers. The observed self-energy effects are in fact well reproduced by models where the charge carriers are coupled to bosonic modes (such as spin fluctuations or phonons) with a cutoff energy of about 0.1 eV.

This analysis confirms our conclusion that the charge carrier response not only exhibits an anomalous narrowing but also loses SW in the SC state. In the framework of a nearest-neighbor tight-binding model, the observed SW loss corresponds to an increase of the kinetic energy in the SC state. Although this trend is in line with the standard BCS theory, as discussed in the introduction, an analysis becomes more difficult beyond this simple approach (*5*, *6*). For instance, correlation effects due to the strong onsite repulsion U of the charge carriers on the Cu ions strongly influence the electronic structure. Within the Hubbard model, a single-band picture becomes inadequate, and the integration should include all Hubbard bands; that is, $\tilde{\Omega} > U$ (*7*, *24*). Changes of the intraband SW unrelated to the kinetic energy may also be associated with structural anomalies known to occur below T_c in a number of high-temperature superconductors, including $YBa_2Cu_3O_{6+x}$ (*25*). Although the expected SW changes due to the T dependence of the lattice parameters are negligible, changes in the relative position of certain ions, such as the apical oxygen ions, may have a significant impact. Finally, the SC-induced broadband SW transfer may be closely related to the so-called pseudogap phenomenon, which has been reported to exist in the cuprate HTSCs even at optimal doping. Within this approach, possible perturbation of the momentum-distribution function over the conduction band due to the coupling of charge carriers to spin fluctuations may contribute to the observed effect. More systematic experimental and theoretical work is needed in order to address these possibilities.

Our broadband (0.01 to 5.6 eV) ellipsometric measurements on $YBa_2Cu_3O_{6.9}$ and $Bi_2Sr_2CaCu_2O_8$ suggest a sizable SC-induced decrease of the total intraband SW. In the context of the nearest-neighbor tight-binding model, this effect implies an increase of the kinetic energy in the SC state, which is in line with the standard BCS theory. We, however, argue that a microscopic understanding of this behavior requires consideration beyond this approach, including strong correlation effects.

References and Notes

1. P. W. Anderson, *The Theory of Superconductivity in the High-T_c Cuprates* (Princeton Univ. Press, Princeton, NJ, 1997).
2. S. Chakravarty, H.-Y. Kee, E. Abrahams, *Phys. Rev. Lett.* **82**, 2366 (1998).
3. J. E. Hirsch, F. Marsiglio, *Phys. Rev. B* **62**, 15131 (2000).
4. M. Tinkham, *Introduction to Superconductivity* (McGraw-Hill, New York, ed. 2, 1996).
5. S. Chakravarty, H.-Y. Kee, E. Abrahams, *Phys. Rev. B* **67**, 100504(R) (2003).
6. M. R. Norman, C. Pépin, *Phys. Rev. B* **66**, 100506(R) (2002).
7. P. F. Maldague, *Phys. Rev. B* **16**, 15131 (1977).
8. Materials and methods are available as supporting material on *Science* Online.
9. A. A. Tsvetkov *et al.*, *Nature* **395**, 360 (1998).
10. D. N. Basov *et al.*, *Science* **283**, 49 (1999).
11. A. V. Boris *et al.*, *Phys. Rev. Lett.* **89**, 4907 (2002).
12. H. J. A. Molegraaf, C. Presura, D. van der Marel, P. H. Kes, M. Li, *Science* **295**, 2239 (2002).
13. A. F. Santander-Syro *et al.*, *Europhys. Lett.* **62**, 568 (2003).
14. M. J. Holcomb, C. L. Perry, J. P. Collman, W. A. Little, *Phys. Rev. B* **63**, 224514 (2001).
15. M. Rübhausen, A. Gozar, M. V. Klein, P. Guptasarma, D. G. Hinks, *Phys. Rev. B* **63**, 224514 (2001).
16. J. Kircher *et al.*, *Physica C* **192**, 473 (1992).
17. S. L. Cooper *et al.*, *Phys. Rev. B* **47**, 8233 (1993).
18. D. L. Feng *et al.*, *Phys. Rev. Lett.* **86**, 5550 (2001).
19. A. E. Karakozov, E. G. Maksimov, O. V. Dolgov, *Solid State Commun.* **124**, 119 (2002).
20. This is most evident if the KK relations are written as

$$\varepsilon_1(\omega) = 1 - 8P\int_0^\omega \frac{\sigma_1(\omega')}{|\omega'^2 - \omega^2|}d\omega' + 8P\int_\omega^\infty \frac{\sigma_1(\omega')}{|\omega'^2 - \omega^2|}d\omega'$$

and combined with the f-sum rule $\int_0^\infty \sigma_1(\omega)d\omega = \text{const.}$
21. D. B. Tanner, T. Timusk, in *The Physical Properties of High Temperature Superconductors III*, D. M. Ginsberg, Ed. (World Scientific, Singapore, 1992), pp. 363–469.
22. An uncertainty of ± 1 in ε_∞ translates into a shift of only about $\pm 0.05\%$ for $\Delta\omega^*_{pl}/\omega^*_{pl}$ and $\Delta\gamma(\omega)/\gamma(\omega)$.
23. The normalized difference is defined as $\Delta f(\omega)/f(\omega) = 2 \times \frac{f(\omega, 100\ K) - f(\omega, 30\ K)}{f(\omega, 100\ K) + f(\omega, 30\ K)}$.
24. J. E. Hirsch, *Phys. Rev. B* **67**, 035103 (2003).
25. V. Pasler *et al.*, *Phys. Rev. Lett.* **81**, 1094 (1998).

26. Supported by the Deutsche Forschungsgemeinschaft (DFG), grant BE2684/1-2 in the consortium FOR538. We gratefully acknowledge Y.-L. Mathis and B. Gasharova for support at the infrared beamline of the Angstroemquelle Karlsruhe (ANKE) at Forschungszentrum Karlsruhe. We also thank O. K. Andersen, E. G. Maksimov, D. N. Aristov, and D. van der Marel for fruitful discussions. We acknowledge B. Nansseu Nako for taking part in some of the measurements.

Supporting Online Material

www.sciencemag.org/cgi/content/full/304/5671/708/DC1
Materials and Methods
Text
Figs. S1 to S6
References and Notes

12 January 2004; accepted 29 March 2004